UNITAS: Tool for supporting evaluation of ship performance in actual seas

by

Naoto SOGIHARA*, Mariko KURODA*, Akiko SAKURADA*, Saori YOKOTA*
and Masaru TSUJIMOTO*

Abstract

Over the past decade, activities for evaluating ship performance in actual seas based on monitored data onboard have been globally implemented. A ship-performance simulator called Vessel Performance Evaluation Tool in Actual Seas (VESTA), which was developed by the National Maritime Research Institute (NMRI), is useful for analyzing monitored data. The analysis requires not only ship principal dimensions but also detailed data such as sectional data or ship performance data obtained from model tests or computations. Preparation of these data is quite difficult for ship owners or operators since they do not have such data.

NMRI developed a tool for supporting evaluation of ship performance in actual seas called United Tool for Assessment of a Ship (UNITAS) to enable ship owners or operators to evaluate ship performance in actual seas in conjunction with monitored data. UNITAS can not only provide hull-form data and estimate ship performance through empirical formulae but also evaluate ship performance in calm seas from monitored data.

UNITAS can provide hull-form data and ship performance based on the ship parameters easily available. This paper describes the outlines of UNITAS and introduces its applications.

＊　Fluids Engineering & Hull Design Department
原稿受付　2019 年 5 月 10 日
審 査 日　2019 年 7 月 3 日

Contents

Nomenclature

$A(i)$: sectional area of i-th section [m^2]
A_E : expanded blade-area ratio [-]
A_L : projected transverse area above water line [m^2]
A_{OD} : projected lateral area of superstructure and cargos on deck (e.g. containers) [m^2]
A_R : projected lateral area of rudders[m^2]
A_T : projected lateral area above water line[m^2]
B : maximum breadth [m]
b_{BK} : breadth of bilge keel [m]
$B(i)/2$: sectional half breadth of i-th section[m]
B_0 : coefficient for interaction between ship and propeller on thrust deduction [-]
C_B : block coefficient [-]
C_{Bdes} : block coefficient at design full condition[-]
C_{B0} : block coefficient calculated from initial C_P curve [-]
C_{WI} : block coefficient calculated from intermediate C_P curve[-]
C_{DIS} : distance from the midship section to the center of projected lateral area (+ means fore from midship) [m]
C_G : coefficient of thrust augmentation due to the interaction between ship hull and propeller [-]
C_M : midship section coefficient [-]
C_N : yaw moment coefficient due to winds [-]
C_P : prismatic coefficient [-]

C_{PA} : prismatic coefficient of aft part (from midship to A.P.) [-]
C_T : propeller loading coefficient [-]
C_{VP} : vertical prismatic coefficient [-]
C_{WA} : water plane area coefficient of aft part (from midship to A.P.) [-]
C_{W0} : water plane area coefficient calculated from initial C_W curve [-]
C_{WI} : water plane area coefficient calculated from intermediate C_W curve [-]
C_X : drag coefficient due to winds[-]
C_Y : lateral force coefficient due to winds[-]
C_0 : coefficient for interaction between ship and propeller regarding wake of ship in model-scale [-]
C_{0s} : coefficient for interaction between ship and propeller regarding wake of ship in full-scale [-]
D : ship depth [m]
d_A : draft at aft [m]
d_{Ades} : d_A at design full condition [m]
d_F : draft at fore [m]
d_{Fdes} : d_F at design full condition [m]
$d(i)$: sectional draft of i-th section [m]
d_M : draft at midship [m]
d_{Mdes} : d_M at design full condition [m]
D_P : propeller diameter [m]
e_a' : bluntness of aft part [-]
e_i : scale effect of wake coefficient [-]
F : fuel oil consumption per day [t/day]
F_{ACT} : F in actual seas [t/day]
F_{CALM} : F in calm seas [t/day]
F_n : Froude number [-]
F_X : longitudinal force due to winds [N]
F_Y : lateral force due to winds[N]
g : acceleration of gravity [m^2/s]
GM : transverse metacentric height [m]
H : significant wave height [m]
H_{BR} : height to bridge top from water line [m]
H_C : height to center of A_L from water line [m]
J : advance coefficient [-]
k : form factor[-]
K_{AW} : non-dimensional added resistance in regular waves [-]
K_{AWc} : non-dimensional added resistance in irregular waves [-]
K_Q : propeller-torque coefficient [-]
K_{Q0} : propeller-torque coefficient in open water[-]
K_T : propeller-thrust coefficient [-]
K_{xx} : transverse radius of gyration [m]
l_{BK} : length of bilge keel [m]
L_{OA} : length overall[m]
L_{PP} : length between perpendiculars [m]
L_{PS} : length between fore position of water line and A.P./aft position of water line [m]
L_R : chord length of rudder [m]
M_Z : yaw moment due to winds[Nm]

MCR : maximum continuous rating [kW]
N_{MCR} : engine revolution at MCR [rpm]
n : propeller revolution [s^{-1}]
n_E : engine revolution [s^{-1}]
OG : height of center of gravity above water line (+ means upside.) [m]
p : aft-bluntness parameter
P_B : braking power [kW]
P_E : effective power [kW]
P/D_P : pitch ratio [-]
R_{AW} : added resistance in regular waves [N]
R_{AWc} : added resistance in irregular waves [N]
r_G : gear ratio [-]
R : resistance in still water with propeller [N]
R_C : resistance in still water with propeller; free-rotating condition [N]
R_T : resistance in calm seas [N]
S_F : wetted surface area of hull [m^2]
S_X : averaged distance between hull and propeller at 70% diameter of propeller [m]
T : thrust [N]
T_w : mean wave period [s]
T_ϕ : natural period of roll [s]
U : relative wind speed [m/s]
U_{a0} : averaged mean inflow velocity at propeller in still water for ship in model-scale [-]
U_{a0s} : averaged mean inflow velocity at propeller in still water for ship in full-scale [-]
u_{ij} : coordinate of the edges of Ferguson-Coons curve [-]
U_w : true wind speed [m/s]
V : ship speed [m/s]
V_{ACT} : ship speed in actual seas [knot]
V_{CALM} : ship speed in calm seas [knot]
V_{des} : designed ship speed [knot]
v_{ij} : vector of tangential line at the edges of Ferguson-Coons curve [-]
V_S : ship speed [knots]
X_{CB} : longitudinal position of the center of buoyancy (+ means fore from midship) [m]
X_G : longitudinal position of the center of gravity (+ means fore from midship) [m]
Z : blade number [-]
ΔF : increase in F in actual seas [ton/day]
ΔV : decrease in V_S in actual seas [knots]
ρ : density of sea water [kg/m^3]
ρ_A : density of air [kg/m^3]
η : propulsive efficiency [-]
η_o : propeller efficiency [-]
η_s : transmission efficiency [-]
η_R : relative rotative efficiency [-]
τ : auxiliary variable in Ferguson-Coons curve [-]
σ_a : flame line factor of aft part [-]
ζ_w : incident wave height [m]
$1\text{-}t$: thrust-deduction coefficient [-]

$1\text{-}t_T$: thrust-deduction coefficient based on R_C [-]
$1\text{-}w_M$: wake coefficient in model-scale [-]
$1\text{-}w_S$: wake coefficient in full-scale [-]

1. Introduction

It is important for both ship operators/owners and shipbuilders to evaluate ship performance in actual seas for reducing greenhouse gas emissions from shipping sectors. Though theoretical or experimental approaches have been conventionally taken for predicting ship performance in actual seas, the evaluation of ship performance based on monitored data through full-scale measurement is spread. To analyze monitored data, it is necessary to prepare various types of ship information such as sectional data, waterplane form, superstructure parameters, and ship-performance parameters in calm seas to which ship operators or owners rarely have access. The evaluation of ship performance in actual seas with sufficient accuracy requires such information.

The National Maritime Research Institute (NMRI) has developed a ship-performance simulator called Vessel Performance Evaluation Tool in Actual Seas (VESTA [1]) that is useful for analyzing monitored data. NMRI also has developed **Uni**ted **T**ool for **A**ssessment of a **S**hip (UNITAS) as a supporting tool for use of VESTA. UNITAS not only provides sectional data using a database of ship types but also estimates performance in calm water such as resistance, self-propulsion factors, and propeller open characteristics (POC). UNITAS also calculates superstructure parameters such as projected area above the waterline to predict added resistance due to winds.

UNITAS extracts a resistance curve and self-propulsion factors in calm seas from monitored data. It also calculates the parameters necessary for predicting self-propulsion factors in waves.

2. Overview

UNITAS was constructed and operated on EXCEL®. The system requirements for the execution of UNITAS are listed in Table 1. The top menu of UNITAS is shown in Fig. 1, and its calculation items are summarized in Table 2.

Calculation buttons are placed in UNITAS for the parameters listed in Table 3. These parameters are calculated with minimal input data from simplified formulae [2].

Table 1 System requirements

Items	Requirements
OS	Microsoft Windows XP / Vista / 7 / 8 / 8.1(32bits / 64bits)
Software	Microsoft EXCEL® 2007 / 2010 / 2013 / 2016
File size	about 38 MB

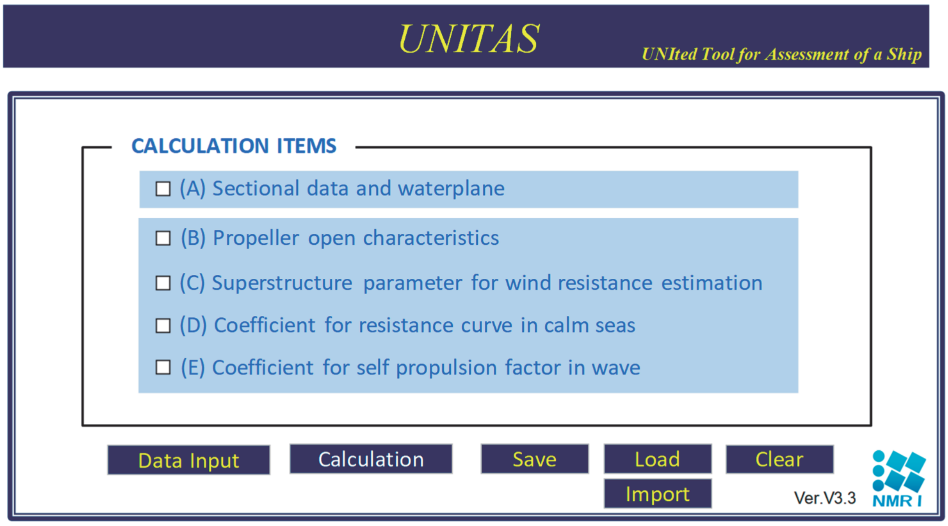

Fig. 1 Top menu of UNITAS

Table 2 Calculation items of UNITAS

	Item	Sub-item	Remarks
(A)	Sectional data and waterplane	(A-1)	Estimation from principal particulars
		(A-2)	Estimation by input of offset data
(B)	Propeller open characteristics	(B-1)	Based on MAU chart
		(B-2)	Based on calculation results of QCM
		(B-3)	Based on propeller design
(C)	Superstructure parameter for wind resistance estimation	None	Using regression formulae based on database
(D)	Coefficient for resistance curve in calm seas	(D-1)	Based on full-scale ship data
		(D-2)	Estimation by empirical formulae
(E)	Coefficient for self-propulsion factor in waves	None	Using regression formulae based on database

Table 3 Parameters calculated from simplified formulae

Parameter	Input
C_{Bdes}	L_{PP}, V_{des}
C_B	L_{PP}, B, d_M, d_{Mdes}, C_{Bdes}
X_{CB}	L_{PP}, C_B, V_{des}, C_{Bdes}
C_P	B, C_B
C_{PA}	L_{PP}, X_{cB}, C_P
D_P	d_{Ades}
A_E	V_{des}, D_P, MCR, N_{MCR}, r_G

3. Calculation items

3.1 Sectional data and waterplane

3.1.1 Estimation from principal particulars

Calculation of ship motion and added resistance in waves requires sectional parameters such as draft, half breadth, and area at each section, waterplane form, as well as ship dimensions. While ship builders can easily apply these data, it is difficult for ship owners or operators to obtain such data. UNITAS provides the sectional parameters and waterplane based on ship principal particulars to which ship owners or operators can access. Specifically, the estimation of the sectional parameters and waterplane requires only L_{PP}, d_M, d_F, d_A, and C_B as input parameters.

UNITAS is provided with offset data of four type ships, i.e., container ship, vehicle carrier, bulk carrier, and tanker, whose principal particulars are listed in Table 4. Sectional draft is calculated based on the profile of the type ships. Unless input C_B is equal to C_B which is calculated using the offset data, C_P and C_W curves are transformed according to the algorithm of the Ferguson-Coons (FC) curve. The FC curve expressed by Eq. (1) is defined by the coordinate and tangential line vector at the edges of the FC curve as illustrated in Fig. 2. The parameters in Eq. (1), x_{ij} and u_{ij} (i, j =1,2), are obtained from the offset data of the type ships. τ in Eq. (1) is an auxiliary variable.

Table 4 Principal particulars of the type ships.

Ship type	container ship	vehicle carrier	bulk carrier	tanker
L_{PP} [m]	300.00	192.00	217.00	324.00
B [m]	40.00	32.26	32.26	60.00
d_{Mdes} [m]	14.00	9.00	12.20	20.50
C_{Bdes}	0.649	0.550	0.840	0.851

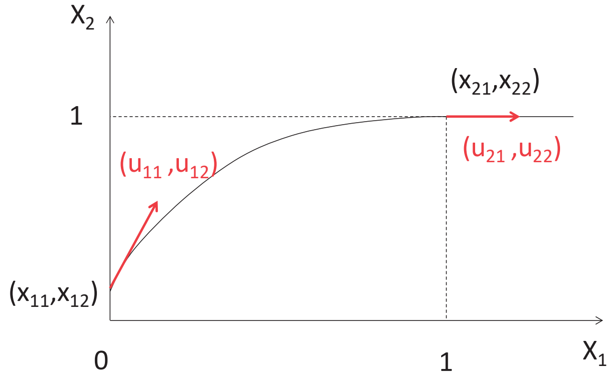

Fig. 2 Ferguson-Coons curve

$$X_1(\tau) = (2x_{11} - 2x_{21} + u_{11} + u_{21})\tau^3 + (-3x_{11} + 3x_{21} - 2u_{11} - u_{21})\tau^2 + u_{11}\tau + x_{11}$$
$$X_2(\tau) = (2x_{12} - 2x_{22} + u_{12} + u_{22})\tau^3 + (-3x_{12} + 3x_{22} - 2u_{12} - u_{22})\tau^2 + u_{12}\tau + x_{12} \quad (1)$$

Figure 3 shows a flowchart of estimating the sectional parameters based on ship principal particulars. The C_P curve is transformed by changing the length of the entrance and that of the run iteratively until the transformed C_P curve satisfies input C_B. After the Cp curve is determined, 'input C_W' C_{WI} is calculated assuming that C_{VP} does not change before and after the transformation. For the C_W curve, similar transformation is conducted until the transformed C_W curve becomes consistent with C_{WI}.

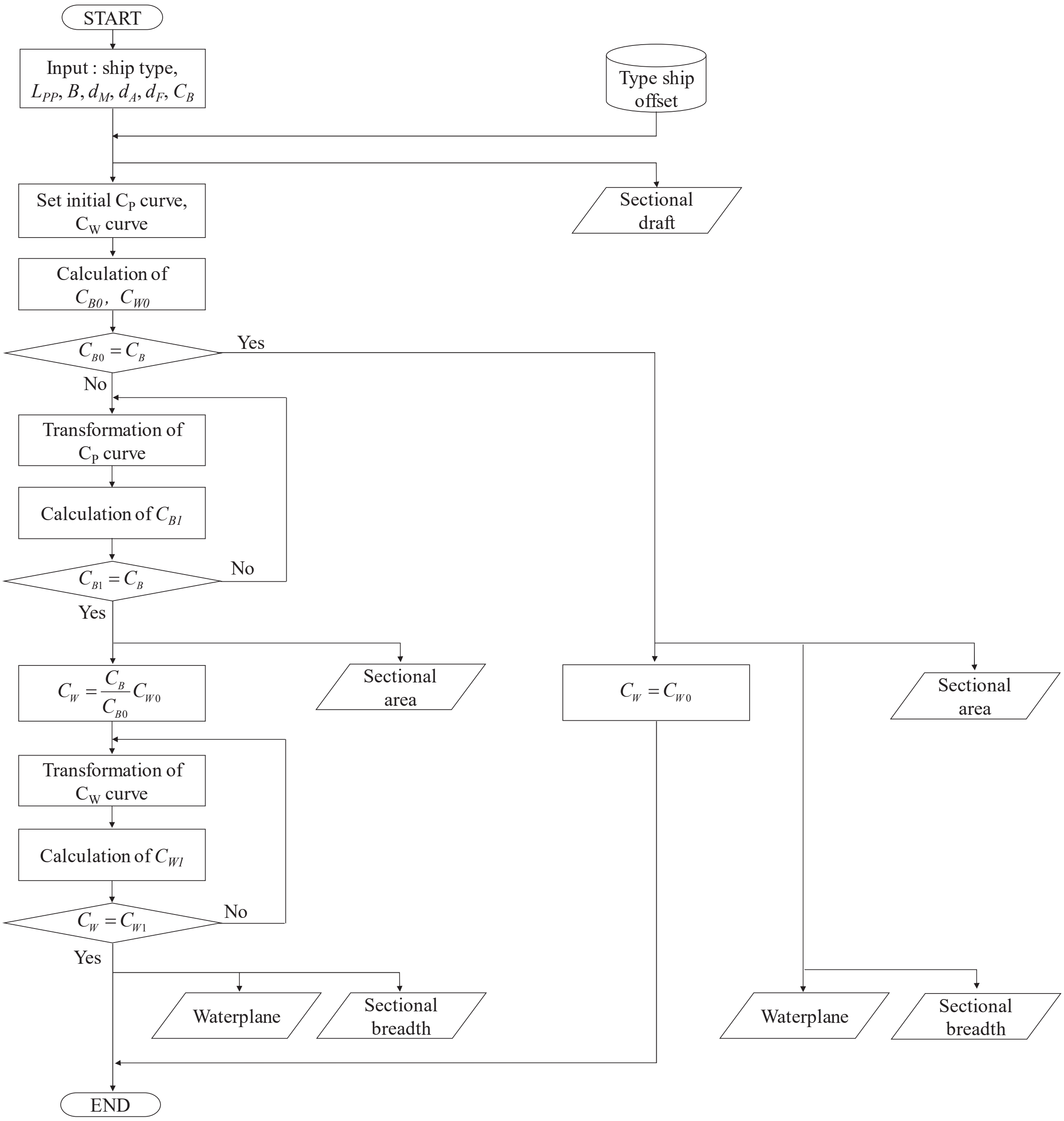

Fig. 3 Flowchart of estimating sectional parameters from principal particulars

3.1.2 Estimation by input of offset data

Users (i.e., owners/operators) having actual offset data for a ship can directly calculate the sectional parameters. The estimation based on the offset data gives more precise sectional parameters. Providing the offset data at any section provides sectional draft, sectional half breadth, and sectional area for any draft condition.

3.1.3 Validation

(1) Sectional data

The effectiveness of the estimation based on the FC curve is validated for the ships listed in Table 5. The ship type for estimating of 33000 DWT chemical tanker (33CT) is assumed to be 'bulk carrier' since C_B of the bulk carrier is nearest that of 33CT. The validation results for the sectional parameters are shown in Figs. 4 to 6, showing good agreement between the sectional parameters estimated based on the FC curve and those estimated using actual offset data.

Table 5 Principal particulars of ships for validation

	33CT	JBC	DTC
Ship type	chemical tanker	bulk carrier	container ship
L_{PP} [m]	170.5	280.0	355.0
B [m]	27.7	45.0	51.0
d_{Mdes} [m]	10.0	16.5	14.5
C_{Bdes}	0.795	0.858	0.661

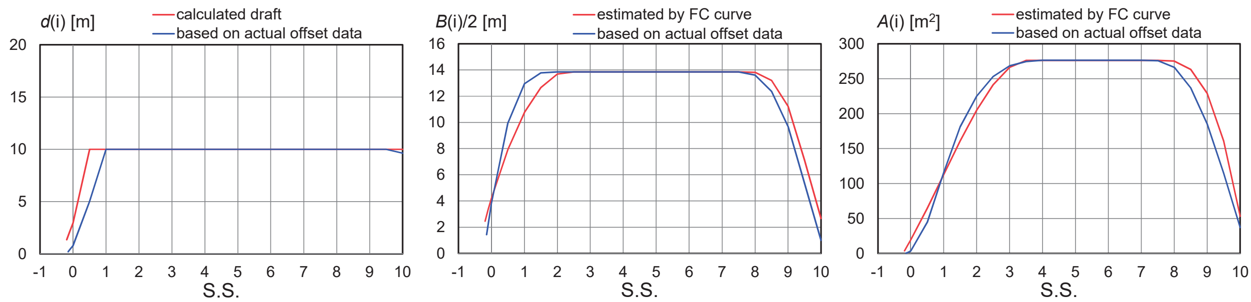

Fig. 4 Validation for sectional parameters of 33CT
(left: draft, center: half breadth, right: sectional area)

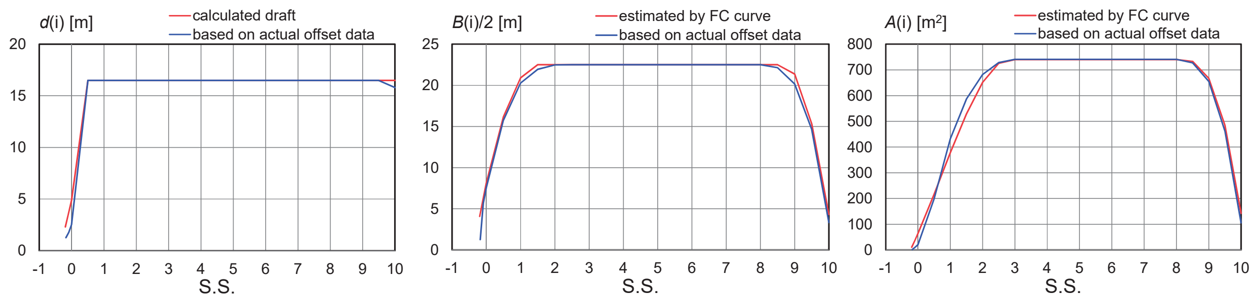

Fig. 5 Validation for sectional parameters of JBC
(left: draft, center: half breadth, right: sectional area)

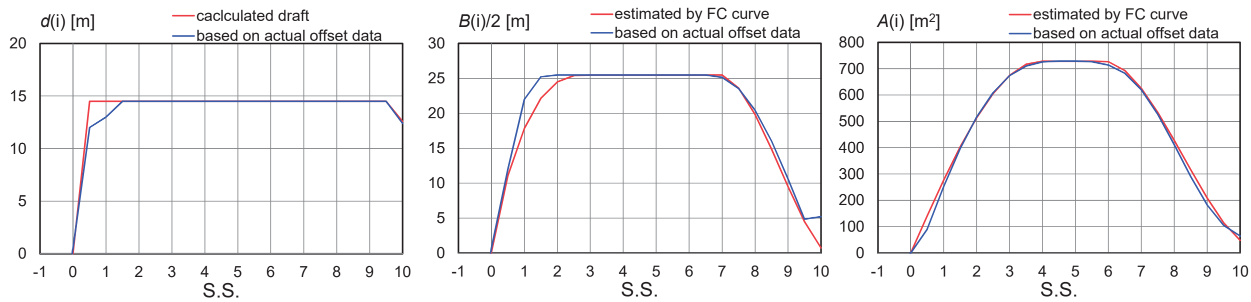

Fig. 6 Validation for sectional parameters of DTC
(left: draft, center: half breadth, right: sectional area)

(2) Added resistance in regular and irregular waves

Added resistance in regular waves is calculated for the ships listed in Table 5. Added resistance in waves is comprised of the component due to ship motion estimated using the New Strip Method and that due to wave reflection at the bow above the waterline. The former is estimated using Maruo's theorem [3] and the latter is calculated according to the method [4] proposed by Tsujimoto et al. Added resistance in regular heading waves K_{AW} defined by Eq. (2) is calculated as shown in Fig. 7.

$$K_{AW} = \frac{R_{AW}}{\rho g \zeta_w^{\ 2} (B^2 / L_{PS})} \tag{2}$$

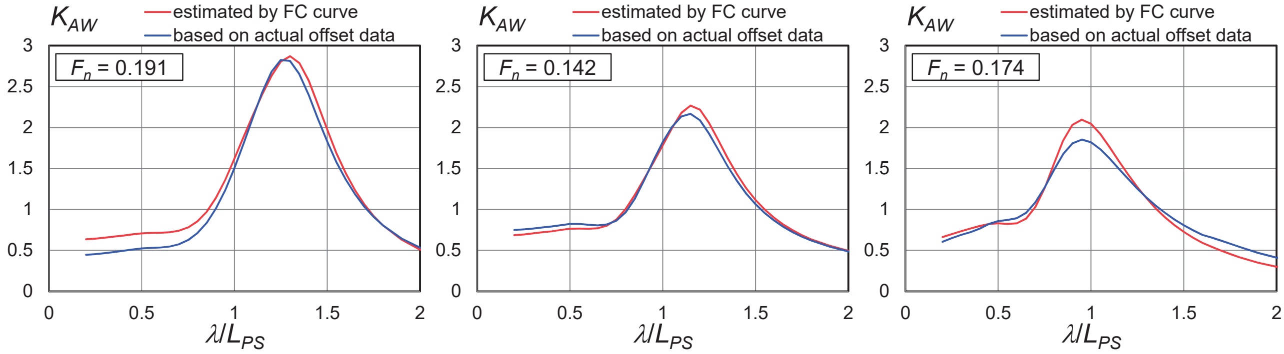

Fig. 7 Added resistance in regular heading waves (left: 33CT, center: JBC, right: DTC)

Waves ships encounter in actual seas are irregular in frequency and direction; therefore, added resistance in short crested irregular waves should be predicted. From this viewpoint, added resistance in such waves is calculated assuming that the directional spectrum is expressed as the product of the frequency spectrum and directional distribution at which IACS spectrum and cosine square power are set, respectively. Added resistance in short crested irregular waves K_{AWc} defined by Eq. (3) is calculated as shown in Fig. 8.

$$K_{AWc} = \frac{R_{AWc}}{8 \rho g H^2 B^2 / L_{PS}} \tag{3}$$

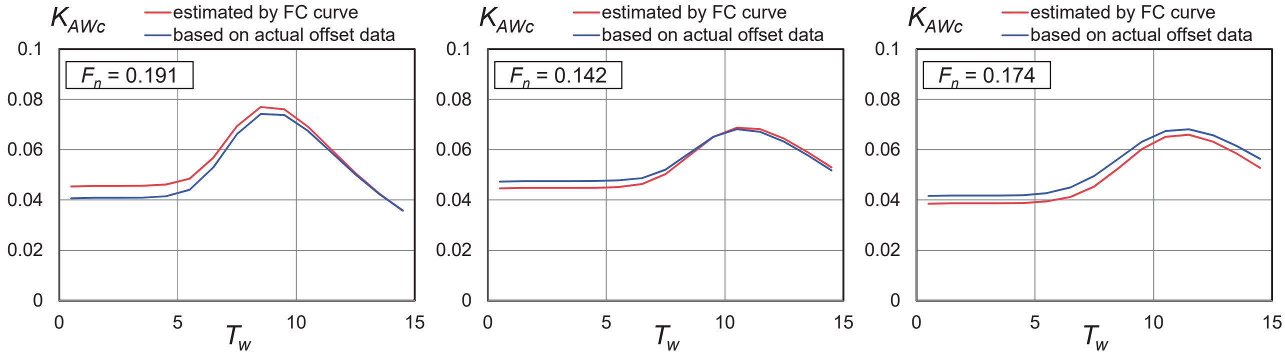

Fig. 8 Added resistance in short crested irregular waves where primary direction is heading
(left: 33CT, center: JBC, right: DTC)

3.1.4 Estimation of roll damping coefficient

In addition to estimating sectional parameters, UNITAS calculates the parameters necessary for estimating roll damping coefficients. The estimation requires the following parameters as well as principal particulars.

- height of center of gravity above waterline OG
- transverse metacentric height GM
- natural period of roll T_ϕ
- wetted surface area S_F
- length of bilge keel l_{BK}
- breadth of bilge keel b_{BK}

OG is calculated using Eq. (4).

$$\overline{OG} = 4.5884\, D \cdot L_{PP}^{\;0.371} - d_M \tag{4}$$

GM is calculated according to Inoue's survey [5] in which it is given by L_{PP} and B for each ship type. T_ϕ is calculated by Eq. (5) which requirestransverse radius of gyration K_{xx}. Although actual K_{xx} should be used for accurate estimation of roll motion, it is not easy to arrange the actual K_{xx}. UNITAS recommends that the non-dimensional transverse radius of gyration K_{xx}/B should be between 0.35 and 0.40.

$$T_\phi = 2\pi \frac{K_{xx}}{\sqrt{g\overline{GM}}} \tag{5}$$

The estimation of S_F follows the paper by Ichinose et al. [6] which originated from Denny's formula and takes into account the frame line of the aft part. l_{BK} is set to be $0.25L_{PP}$, and b_{BK} is estimated geometrically with the sectional area at midship.

3.2 Propeller open characteristics

To evaluate ship performance in actual seas, it is necessary to prepare propeller open characteristics (POC) in full-scale. UNITAS uses three approaches for estimating POC.

(1) Based on MAU chart

(2) Based on QCM (Quasi-Continuous vortex lattice Method)

(3) Based on propeller design

Approaches (1) and (2) require only pitch ratio P/D_P, expanded area ration A_E, and blade number Z. These are interpolations of the database of the MAU chart and QCM simulation, respectively. The range of the database is shown in Table 6. Approaches (1) and (2) include practical full-scale correction which provides 1% improvement in thrust and torque coefficients. If the parameters required in the approaches (1) and (2) cannot be used, approach (3) is used, which requires propeller diameter and draft at the design full condition. The effectiveness of these approaches is summarized in Figs. 9 to 11 for 499GT cargo ship, 33CT, and DTC, respectively. These figures show that all three approaches effectively estimate POC.

Table 6 Range of database of MAU chart and QCM simulation

	MAU chart		QCM simulation	
blade number	pitch ratio	expanded area ratio	pitch ratio	expanded area ratio
3	0.6~2.2	0.30~1.10	none	
4	0.6~1.6	0.40~0.70		0.30~0.70
5	0.4~1.6	0.50~1.10	0.6~1.2	0.35~1.10
6	0.5~1.5	0.55~0.85		0.55~1.15

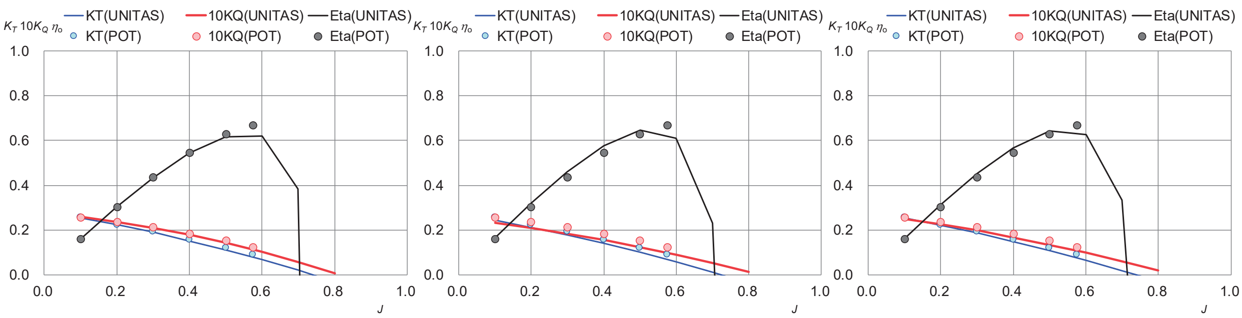

Fig. 9 Validation for POC of 499GT cargo ship

(left: Based on MAU chart, center: Based on QCM, right: Based on propeller design)

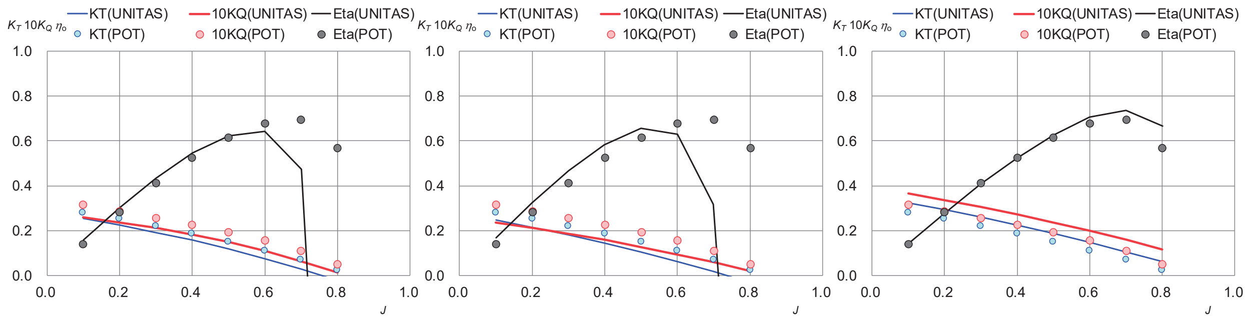

Fig. 10 Validation for POC of 33CT
(left: Based on MAU chart, center: Based on QCM, right: Based on propeller design)

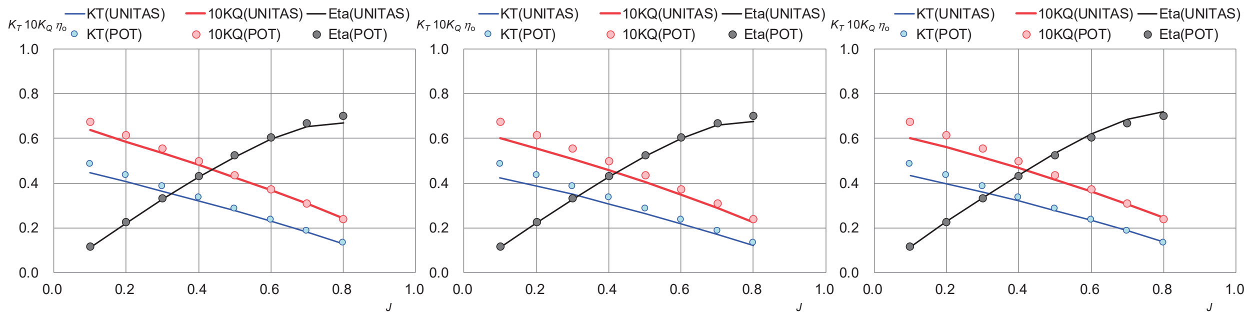

Fig. 11 Validation for POC of DTC
(left: Based on MAU chart, center: Based on QCM, right: Based on propeller design)

3.3 Superstructure parameters for wind resistance estimation

Wind resistance should be accurately estimated for evaluating ship performance in actual seas. While wind resistance is measured in wind tunnel tests, formulae for predicting wind resistance has been proposed (e.g. Fujiwara's method [7]). Such prediction requires the superstructure parameters illustrated in Fig. 12. These parameters should be given by a general arrangement of a ship (GA).

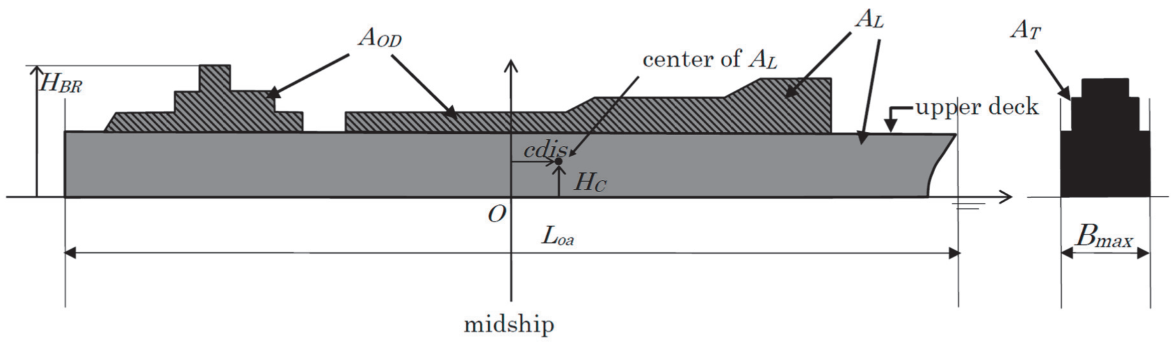

Fig. 12 Superstructure parameters

UNITAS calculates the superstructure parameters according to the method developed by Kitamura et al [8], which is based on the actual superstructure parameters of container ships, vehicle carriers, bulk carriers, and tankers on which wind tunnel tests were carried out. The method expresses the superstructure parameters as a 1st-order regression formula of L_{OA} and B. UNITAS updated the form of this regression formula and its coefficients for container ships and bulk carriers to cover large ships by adding the superstructure parameters of mega-container ships and cape-size bulk carriers for full condition. The size ranges of container ships and bulk carriers are listed in Table 7.

Table 7 Size ranges of container ships and bulk carriers

ship type	number of ships	range of L_{OA} [m]	range of B [m]
container ship	14	119-400	19-59
bulk carrier (full)	10	141-330	19-57

The updated regression formula is expressed in Eq. (6). Parameter P indicates A_T, A_L, A_{OD}, C_{DIS}, H_{BR}, and H_C. Parameter X has three forms: P(raw value), P/L_{OA}, and P/B. The coefficients of the updated formula are listed in Table 8. Figs. 13 and 14 indicate the comparison between the true values and the estimated values using the updated regression formula for container ships and bulk carriers in full condition, which shows good agreement except C_{DIS}.

$$X = aB + bL_{OA} + c$$
$$X = \begin{cases} P & form:1 \\ P/L_{OA} & form:2 \\ P/B & form:3 \end{cases} \tag{6}$$

Table 8 Coefficients for updated regression formula for container ships and bulk carriers

ship type	P	A_T	A_L	A_{OD}	C_{DIS}	H_{BR}	H_C
container ship	*form*	3	2	2	1	1	1
	a	8.047E-03	5.810E-01	2.905E-01	4.102E-01	6.503E-01	1.526E-01
	b	8.059E-02	1.598E-02	2.817E-02	-8.361E-02	3.207E-02	3.312E-02
	c	1.031E+01	-2.138E+00	-5.280E+00	-2.627E+00	2.995E+00	-5.348E-01
bulk carrier (full)	*form*	1	1	1	1	1	1
	a	2.377E+01	7.127E+01	1.401E+01	2.575E-01	7.025E-01	3.562E-03
	b	-1.273E+00	-1.087E+00	2.984E-01	-1.017E-01	-3.311E-02	1.468E-02
	c	8.369E+01	1.407E+02	1.422E+02	3.157E+00	7.549E+00	4.097E+00

The updated regression formula is validated by comparing the estimation by Fujiwara's method and results of wind tunnel tests [9] for container ships ($L_{OA} = 312$) and JBC ($L_{OA} = 291.2$) given in Table 4. The comparisons on C_X, C_Y, and C_N , which are defined in Eqs. (7) to (9), are shown in Figs. 15 and 18 for a container ship, JBC in full condition, vehicle carrier, and 33CT, respectively, where zero degree means the heading for wind angle and a positive value means thrust for C_X. Figures. 15 to 18 include estimations based on the actual superstructure parameters (denoted with 'VESTA') and results of wind tunnel tests (denoted with 'Exp.') and show that, although estimation of C_N should be improved, the superstructure parameters obtained from the updated regression formula can predict wind resistance with practical accuracy.

$$C_X = \frac{F_X}{0.5\rho_A U^2 A_T} \tag{7}$$

$$C_Y = \frac{F_Y}{0.5\rho_A U^2 A_L} \tag{8}$$

$$C_N = \frac{M_Z}{0.5\rho_A U^2 A_L \cdot L_{OA}} \tag{9}$$

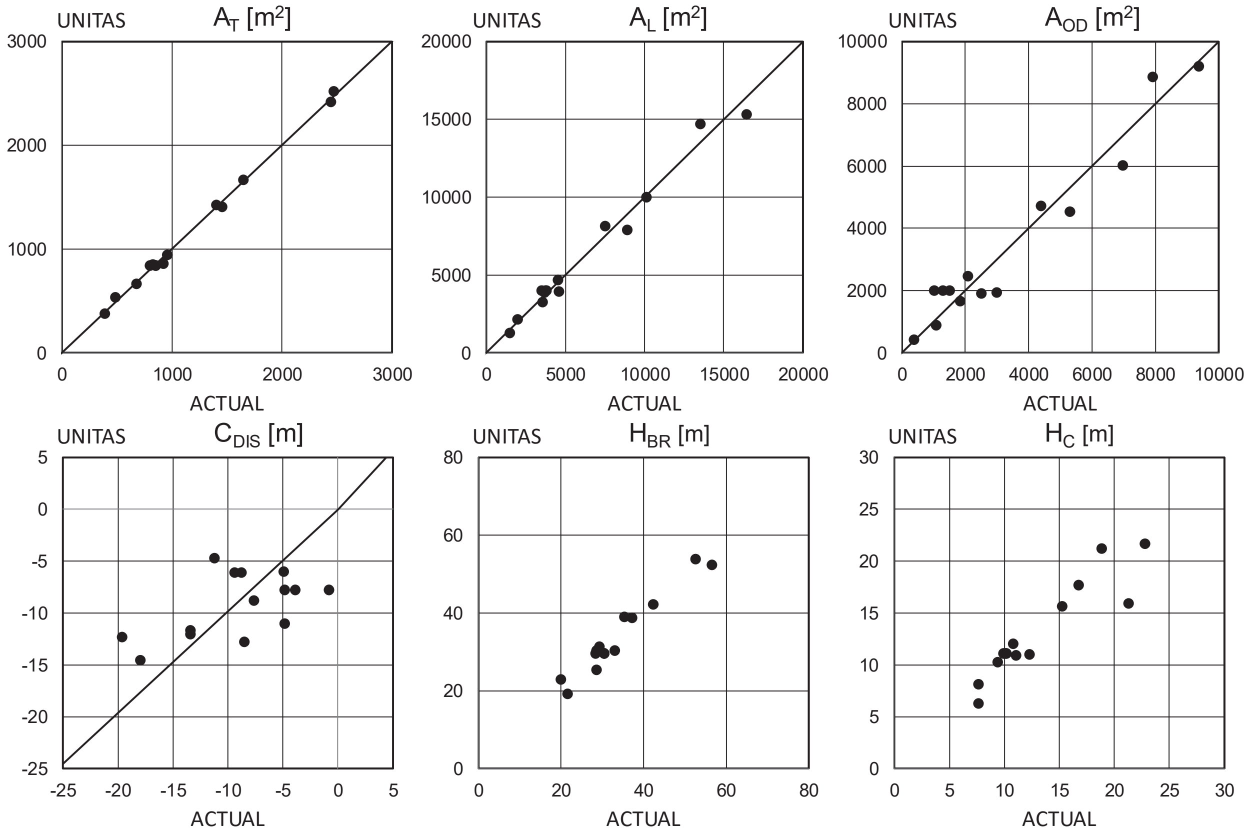

Fig.13 Comparison of superstructure parameters (container ships)

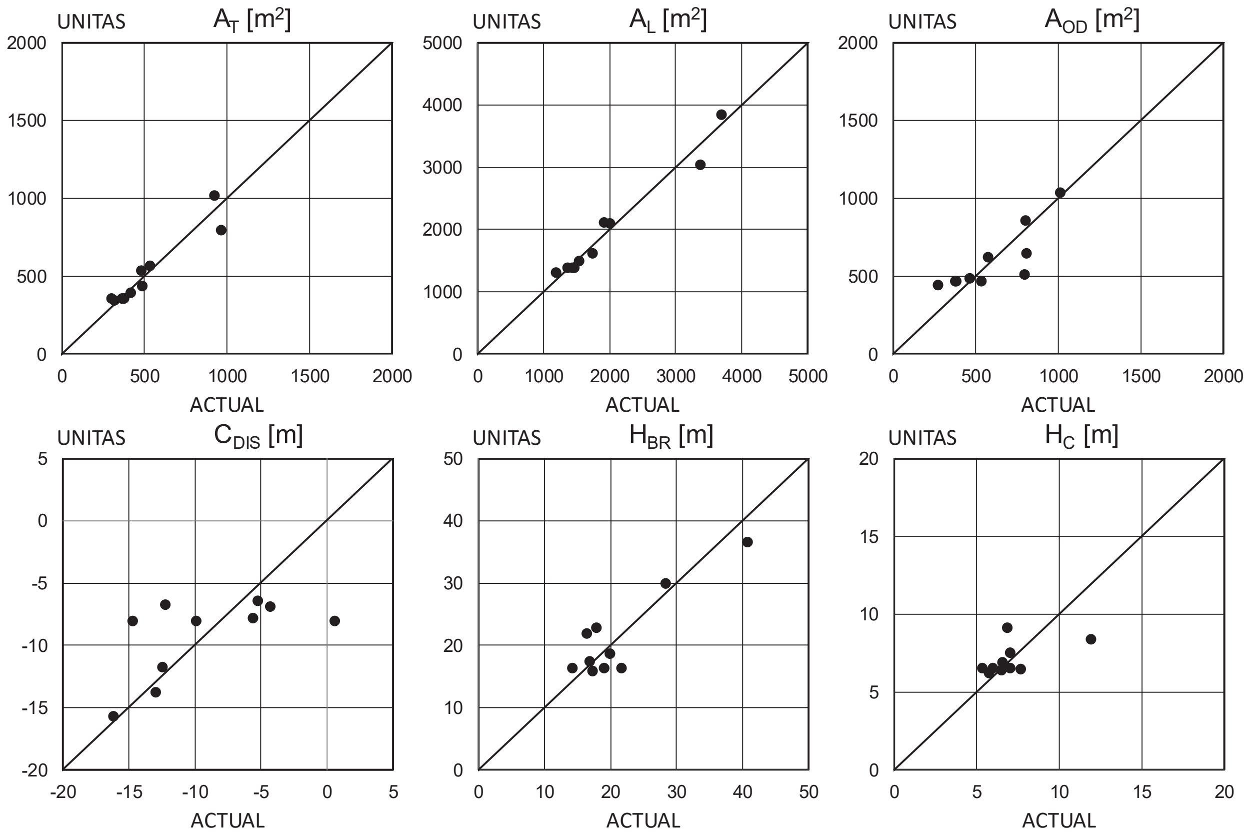

Fig.14 Comparison of superstructure parameters (bulk carriers in full condition)

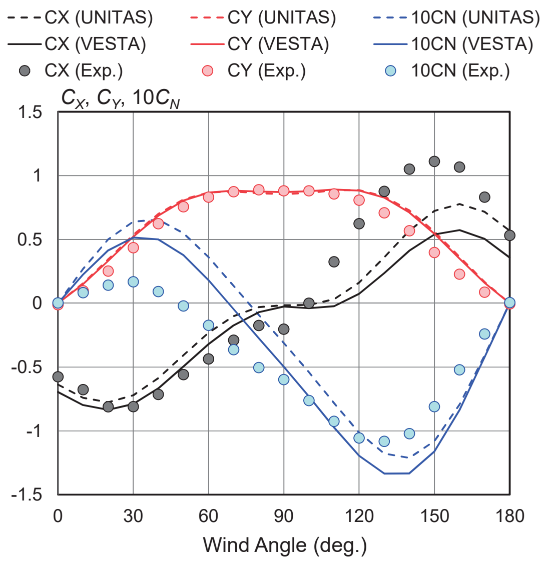

Fig. 15 Validation for container ship (L_{OA} = 312 m)

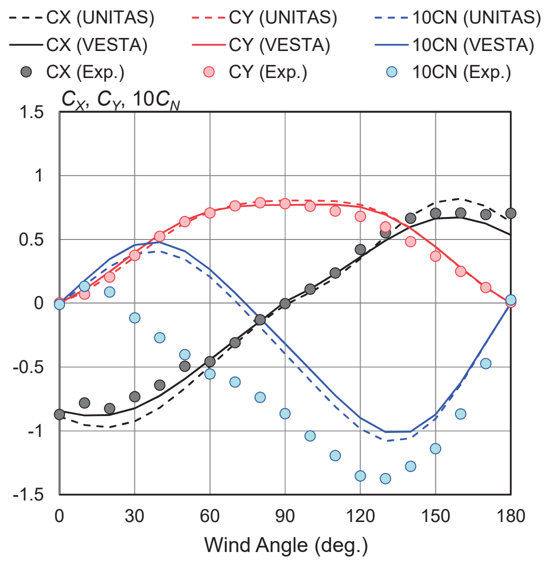

Fig. 16 Validation for JBC (L_{OA} = 291.2 m)

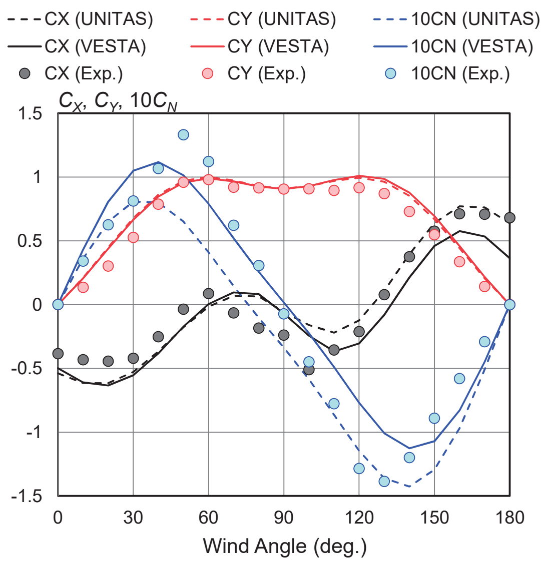

Fig. 17 Validation for vehicle carrier (L_{OA} = 199 m)

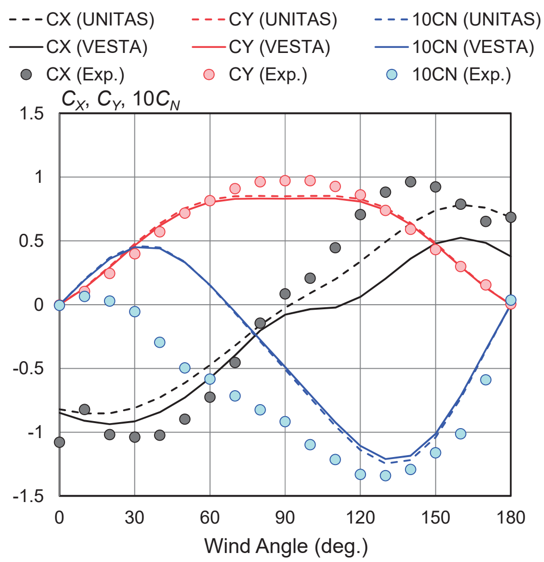

Fig. 18 Validation for 33CT (L_{OA} = 178 m)

3.4 Coefficients for resistance curve in calm seas

3.4.1 Based on full-scale ship data

Since the resistance curve in calm seas is fundamental the evaluating ship performance in actual seas, it should be obtained with sufficient accuracy. However, it is difficult to obtain the resistance curve under every draft condition in operation. Therefore, it is appropriate to extract the resistance curve and self-propulsion factors in calm seas from full-scale ship data. The dataset of ship speed V, engine revolution n_E, and braking power P_B is necessary for estimating the resistance curve.

The estimation of the resistance curve and self-propulsion factors in calm seas follows the thrust-identified method. Propeller torque coefficient in full-scale K_Q and that in open water K_{Q0} are calculated using Eqs. (10) to (12), respectively.

$$K_Q = \frac{P_B \eta_S}{2\pi \rho n^3 D_P^{\,5}} \tag{10}$$

$$n = r_G n_E \tag{11}$$

$$K_{Q0} = \eta_R K_Q \tag{12}$$

Advance coefficient J and propeller thrust coefficient K_T corresponding to K_{Q0} are given by POC. The obtained J gives the wake coefficient in full-scale 1-w_S and the propeller efficiency η_o using Eqs. (13) and (14).

$$1 - w_S = \frac{nD_P J}{V} \tag{13}$$

$$\eta_O = \frac{K_T J}{2\pi K_{Q0}} \tag{14}$$

Thrust deduction coefficient 1-t and propeller rotative efficiency η_R should be used based on model tests or CFD simulation; otherwise, such data are not available, the following formula [6] shown in Eqs. (15) to (18) can be used. Rudder chord length L_R in Eq. (15) can be estimated using the empirical formula [2].

$$1 - t = 1 - \left[0.7\tan^{-1}\left(\left(\frac{0.8}{0.8 + S_X} \right)^{1.31} \right) - 0.02 \right] - 3.1301 \frac{L_R D_P}{L_{PP} d_M} \tag{15}$$

$$S_X = \frac{0.3}{(p + 0.26)^{1.35}} + 0.3 \tag{16}$$

$$p = \frac{C_M}{L_{PP}\sqrt{C_B / Bd_M}} \times \frac{B/L_{PP}}{1 - C_{PA}} \tag{17}$$

$$\eta_R = -43.0p^3 + 8.0p^2 + 1.0 \tag{18}$$

Accordingly, propulsive efficiency η and effective power P_E are calculated using Eqs. (19) and (20).

$$\eta = \frac{1 - t}{1 - w_S} \eta_R \eta_O \eta_S \tag{19}$$

$$P_E = \eta P_B \tag{20}$$

Resistance in calm seas is estimated from P_E. For realistic estimation of resistance in calm seas, wind resistance due to self-running should be eliminated, which is achieved using Eq. (21).

$$\frac{R_T}{0.5\rho L_{PP} d_M} = \frac{1}{0.5\rho L_{PP} d_M} \left(\frac{P_E}{V} + \frac{\rho_A A_T C_X V^2}{2} \right) \tag{21}$$

The above analysis means that the parameters, resistance and wake coefficient, are extracted from the data collected through performance monitoring. The extracted parameters are continuously accumulated and construct the database of propulsion performance in calm seas. Formulation on the parameters by displacement can predict ship performance under any draft condition [10], which can contribute to voyage planning.

3.4.2 Estimation by empirical formulae

The resistance curve and self-propulsion factors are estimated with ship principal particulars by using the empirical formulae used in a program “HOPE” [6], which is available if the monitored data is not available. The comparison on $1\text{-}w_S$ and P_B between ‘Based on full-scale ship data’ and ‘Estimation by empirical formulae’ is shown in Fig. 19 and Fig. 20 for a container ship and a vehicle carrier, respectively. Though $1\text{-}w_S$ has a gap between the both which is derived from the estimation of POC, the empirical formulae in HOPE can estimate ship performance in calm seas with practical accuracy.

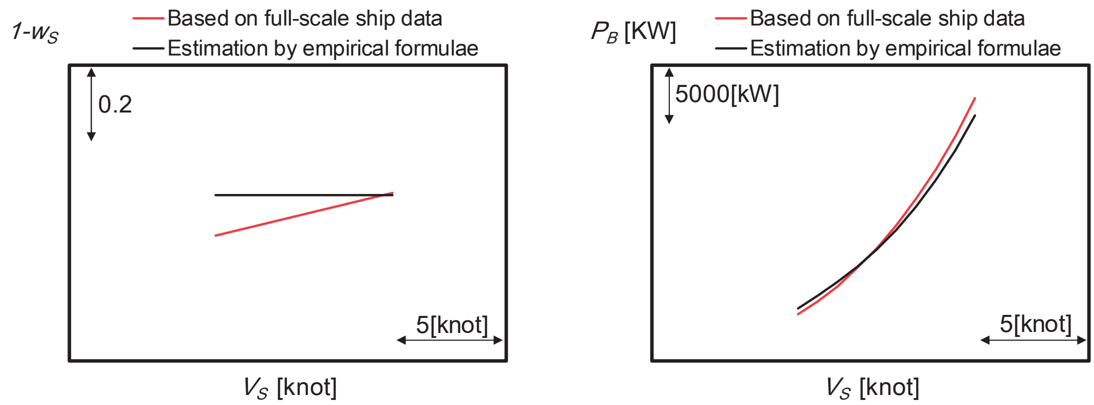

Fig. 19 Comparison between ‘Based on full-scale ship data’ and ‘Estimation by empirical formulae’ for a container ship (L_{PP} = 300 m)

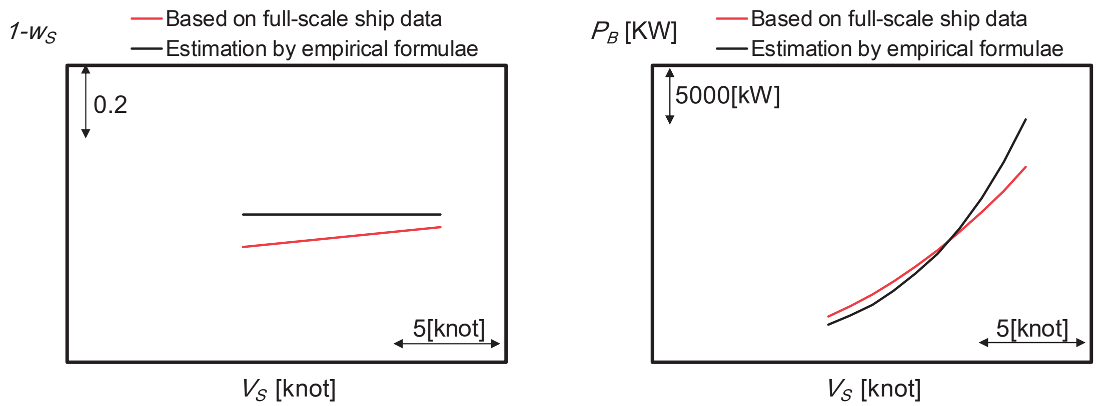

Fig. 20 Comparison between ‘Based on full-scale ship data’ and ‘Estimation by empirical formulae’ for vehicle carrier (L_{PP} = 192 m)

3.5 Coefficients for self-propulsion factors in waves

3.5.1 Load variation method

VESTA applies the load variation method [11-12] to predict self-propulsion factors in waves [13]. The key parameters for the load variation method are propeller loading coefficient C_T and coefficient of thrust augmentation due to the interaction between ship hull and propeller C_G, defined by Eqs. (22) and (23), respectively. R_C in Eq. (23) is resistance in still water with propeller under free-rotating condition and is given as R at T=0.

$$C_T = \frac{T}{\frac{1}{2}\rho V^2 \frac{\pi D_P^2}{4}} \tag{22}$$

$$C_G = \frac{R + T - R_C}{\frac{1}{2}\rho V^2 \frac{\pi D_P^2}{4}} \tag{23}$$

C_G and effective wake coefficient 1-w_M are expressed byEqs. (24) and (25), respectively. These equations contain three coefficients: B_0, C_0, and U_{a0}, which are determined from load variation tests. B_0 expresses the interaction between ship and propeller on thrust deduction, C_0 expresses the interaction between ship and propeller regarding the wake of ship, and U_{a0} expresses the averaged mean inflow velocity at the propeller in still water. Using R_C as ship resistance in still water provides thrust deduction coefficient 1-t_T, as shown in Eq. (26).

$$C_G = B_0\left(-U_{a0} + \sqrt{C_T + U_{a0}^2}\right) \tag{24}$$

$$1 - w_M = U_{a0} + C_0\left(-U_{a0} + \sqrt{C_T + U_{a0}^2}\right) \tag{25}$$

$$1 - t_T = 1 - \frac{C_G}{C_T} \tag{26}$$

3.5.2 Regression formulae for estimating coefficients in load variation method

UNITAS calculates the coefficients with ship principal particulars using regression formulae (Eqs. (27) to (32)), which were developed on the basis of model tests with the ships listed in Table 9. The comparison of the coefficients in Fig. 21 shows that the estimated coefficients have good correlation with those obtained from model tests.

For the chemical tanker (33CT) shown in Table 5, the comparison of the coefficients and that of 1-w_M and 1-t_T between UNITAS and the model tests are shown in Table 10 and Fig. 22, respectively, which shows that UNITAS has practical accuracy in estimating of 1-w_M and 1-t_T. based on the load variation method.

Table 9 Ships used for regression formulae

Ship	condition	L_{PP}	B	d_M	F_n
container	full	300.0	40.0	14.0	0.225
vehicle carrier-A	scantling	192.0	32.2	10.0	0.190, 0.213, 0.237
vehicle carrier-B	full	190.0	32.2	9.0	0.203, 0.238
	ballasted			7.6	0.203
bulk carrier-A	full	160.0	27.0	9.7	0.150, 0.180
bulk carrier-B	scantling	186.0	32.2	12.5	0.143, 0.155, 0.167, 0.179
	ballasted			5.6	0.159, 0.170, 0.183, 0.195
tanker	full	324.0	60.0	20.5	0.160
	ballasted			8.5	0.172
domestic general cargo of 499GT	full	75.0	12.0	4.1	0.203

$$B_0 = 0.746 - 0.027 \cdot \frac{L_{PP}}{B} - 1.373 \cdot C_{PA} + 0.865 \cdot C_B - 0.023 \cdot e_a' + 0.394 \cdot F_n \tag{27}$$

$$C_0 = -0.800 + 0.002 \cdot \frac{L_{PP}}{B} + 1.145 \cdot C_{PA} + 0.018 \cdot C_B + 0.095 \cdot e_a' - 1.077 \cdot F_n$$

(28)

$$U_{a0} = 5.917 + 0.264 \cdot \frac{L_{PP}}{B} - 6.715 \cdot C_{PA} - 0.485 \cdot C_B - 0.577 \cdot e_a' - 0.147 \cdot F_n - 0.155 \cdot k \tag{29}$$

$$k = 1.698 + 0.048\sigma_a - 0.113 e_a' - 19.056 \frac{C_B}{L_{PP}/B} + 76.14 \left(\frac{C_B}{L_{PP}/B} \right)^2 \tag{30}$$

$$e_a' = \frac{L_{PP}/B}{\sqrt{0.25 + (d_M/B)^2}} (1 - C_{PA}) \tag{31}$$

$$\sigma_a = \frac{1 - C_{WA}}{1 - C_{PA}} \tag{32}$$

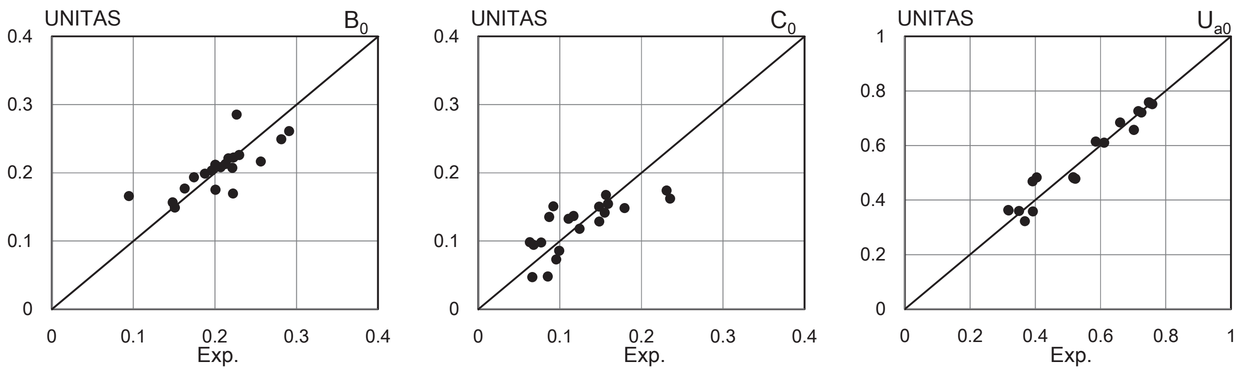

Fig. 21 Comparison of coefficients in load variation method

Table 10 Comparison on the coefficients for 33CT between UNITAS and model tests

	B_0	C_0	U_{a0}
model tests	0.2625	0.1154	0.6223
UNITAS	0.2685	0.1036	0.5887

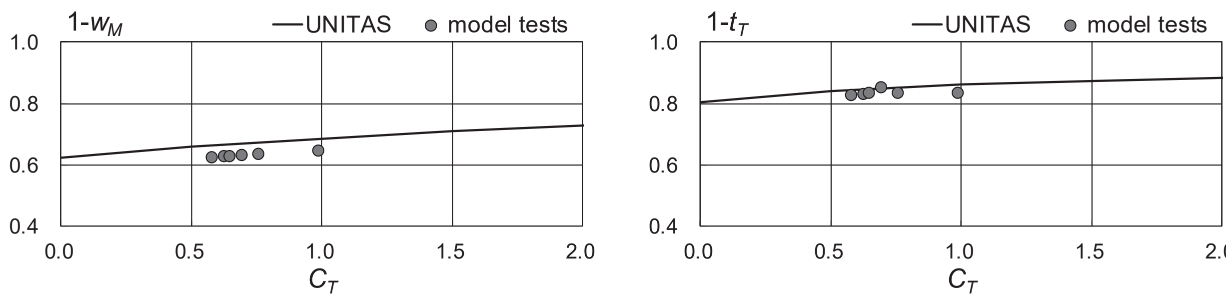

Fig. 22 Comparison of 1-w_M and 1-t_T for 33CT between UNITAS and model tests

3.5.3 Scale up to full-scale

It is well-known that the wake coefficient in full-scale is larger than that in model-scale. The wake coefficient in full-scale is estimated as follows; replacing 1-w_M in Eq. (25) with 1-w_S obtained by Eq. (33) yields C_{0s} and U_{a0s}, which means C_0 and U_{a0} in full-scale, respectively.

$$1 - w_S = (1 - w_M) \cdot e_i \tag{33}$$

where e_i indicates the scale effect of the wake coefficient and obtained by Yazaki's formula [14] in UNITAS.

4. Application

Performance prediction in actual seas was conducted for the chemical tanker (33CT) shown in Table 10 to discuss the effectiveness of the parameters estimated by the method described in Section 3. Ship performance in actual seas cam be predicted according to Tsujimoto et al., [1] who deals with a ship navigating in steady conditions. Solving the equilibrium equations of forces acting on a ship yields power curves in actual seas. The ship speed, engine revolution, engine power, and fuel oil consumption (FOC) in actual seas can be calculated in conjunction with the engine characteristics.

The decrease in ship speed (ΔV) and increase in F (ΔF), which are defined in Eqs. (34) and (35), respectively, are calculated in heading waves and winds with constant n_E. The performance prediction applies the resistance curves in calm seas by the approaches described in section 3.4. The MCR of the engine and the engine revolution at MCR are 7900 kW and 101.88 rpm, respectively. The specific fuel oil consumption (SFC) is shown in Fig. 23. The sea condition for this performance simulation was based on the Beaufort scale and set as indicated in Table 11. Wind waves were considered in the prediction whilst swells were not considered.

$$\Delta V = V_{CALM} - V_{ACT} \tag{34}$$

$$\Delta F = F_{ACT} - F_{CALM} \tag{35}$$

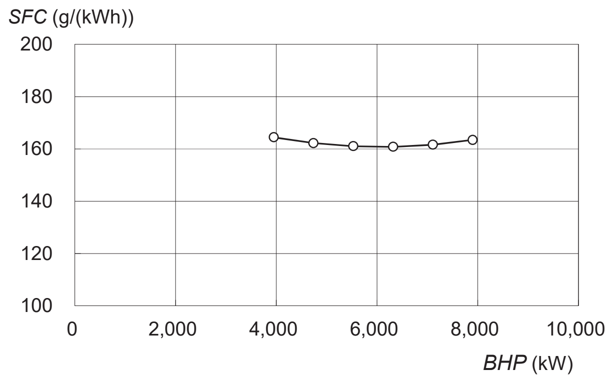

Fig. 23 Specific fuel oil consumption (SFC) of engine

Table 11 Sea condition for performance prediction

True wind speed U_w [m/s]	Significant wave height H [m]	Mean wave period T_w [s]
4.4	0.6	3.0
6.9	1.0	3.9
9.8	2.0	5.5
12.6	3.0	6.7
15.7	4.0	7.7

The results of this simulation are shown in Figs. 24 and 25, showing ship speed and fuel oil consumption, respectively. In these figures, ‘ACTUAL’ means the result based on actual parameters such as sectional data, superstructure parameters, and performance parameters obtained from model tests. ‘UNITAS’ indicates the results based on the estimated parameters from the method described in section 3.4. ‘UNITAS with model test B0, C0, Ua0’ means the results based on the estimated parameters and coefficients B_0, C_0, and U_{a0} obtained from model tests.

Figure 24 shows that there is a gap between the prediction based on the estimated hull-form and performance parameters and that based on the actual parameters. Figure 24 also indicates that V and F at $H = 0$ are differed between ‘ACTUAL’ and ‘UNITAS’. Application of B_0, C_0, and U_{a0} obtained from load variation tests to ‘UNITAS’ improved prediction of V and F as shown in Fig. 24. Consequently, the formulae for B_0, C_0, and U_{a0} should be improved for more accurate prediction of ship performance in actual seas.

Figure 25 shows that ΔV and ΔF are well-estimated based on the method described in section 3.4, which concludes that the parameters required for the estimation of added resistance in waves and that in winds enable accurate prediction of ship performance in actual seas.

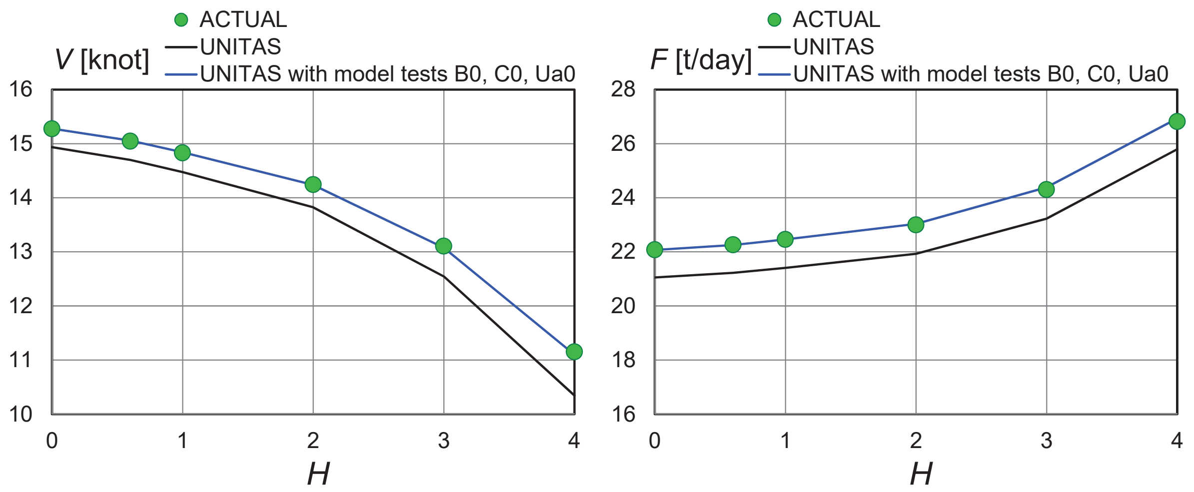

Fig. 24 Results of ship performance simulation (left: ship speed (V) , right: FOC per day (F))

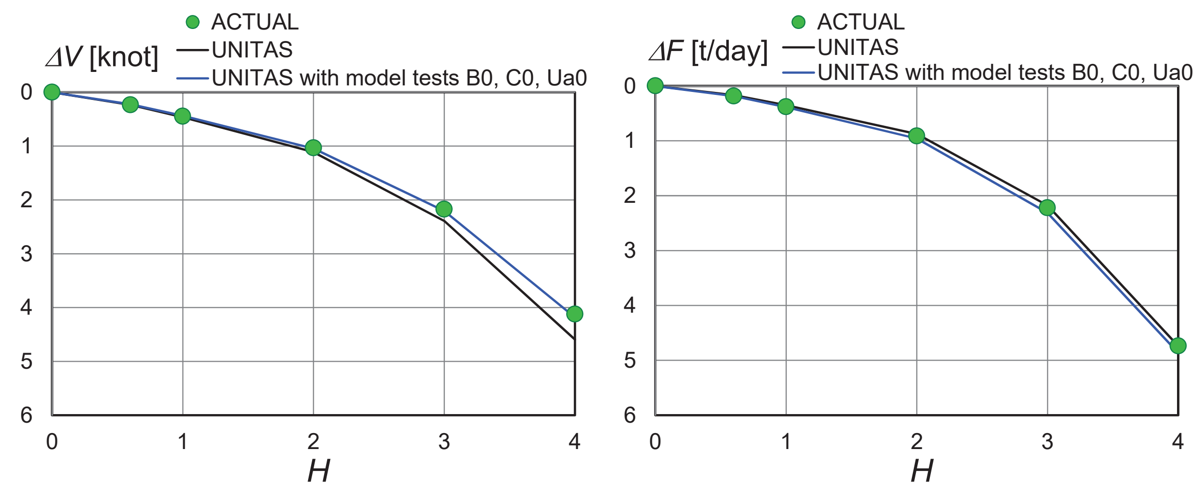

Fig. 25 Results of ship performance simulation.
(left: decrease in ship speed (ΔV), right: increase in FOC per day (ΔF))

5. Concluding remarks

This paper outlines UNITAS, a tool supporting the evaluation of ship performance in actual seas and introduces methods that UNITAS applies for estimating the parameters necessary for such evaluation. The methods for estimating the parameters are validated by comparing with the true values and the results from model tests and conducting simulation of ship performance in actual seas with the estimated parameters. Finally, this paper shows that, though the coefficients in load variation method should be improved, the methods applied to UNITAS have sufficient accuracy to evaluate the performance with accuracy.

The authors believe that UNITAS is helpful in evaluating ship performance in actual seas.

References

1) M. Tsujimoto, N. Sogihara, M. Kuroda, and A. Sakurada: Development of a Ship Performance Simulator in Actual Seas, Proceedings of the ASME 2015 34th International Conference in Ocean, Offshore and Arctic Engineering, OMAE2015-41708, 2015.
2) M. Tsujimoto, M. Kuroda, N. Sogihara, and A. Sakurada: Development of Empirical Formulae for Estimating Ship Performance, Papers of National Maritime Research Institute, Vol. 18, No. 3, pp. 91-106, 2018.
3) H. Maruo: Resistance in Waves, Research on Seakeeping Qualities of Ships in Japan, the Society of Naval Architects of Japan, Vol. 8, pp. 67-102, 1963.
4) M. Tsujimoto, K. Shibata, M. Kuroda, and K. Takagi: A Practical Correction Method for Added Resistance in Waves, Journal of the Japan Society of Naval Architects and Ocean Engineering, Vol. 8, pp. 141-146, 2008.
5) Y. Inoue, K. Okuzumi, S. Itatsu, T. Hayashi, and N. Hikasa: Shipform Characteristics and Motion Responses in Seaway of Various Cargo Ships (in Japanese), Journal of the Kansai Society of Naval Architects, No. 208, pp .11-25, 1988.
6) Y. Ichinose and K. Kume: A Program named “HOPE Light” for Optimizing Hull-Form Dimensions (in Japanese), Papers of National Maritime Research Institute, Vol. 15, No. 4, pp. 13-25, 2016.
7) T. Fujiwara, M. Ueno and Y. Ikeda: Cruising performance of a large passenger ship in heavy sea, Proceedings of Sixteenth International Offshore and Polar Engineering Conference, pp. 304-311, 2006.
8) F. Kitamura, M. Ueno, T. Fujiwara, and N. Sogihara: Estimation of above water structural parameters and wind loads on ships, Journal of Ships and Offshore Structures, Vol. 12, No. 8, pp. 1100-1108, 2017. http://www.tandfonline.com/doi/full/10.1080/17445302.2017.1316556
9) K. Kume, H. Ohba, H. Orihara, and S. Mizokami: Wind Velocity Profile and Representative Wind Velocity for Wind Resistance Measurement of Ship Models, Journal of Japan Society of Naval Architecture and Ocean Engineering, (in submission)
10) N. Sogihara, A. Sakurada, M. Kuroda, M. Tsujimoto, Y. Sugimoto, and K. Hasegawa: Development of A Numerical Model on Displacement Correction for Ship Performance in Calm Seas Based on Full-Scale Measurement, Proceedings of Twenty-ninth International Offshore and Polar Engineering Conference, pp. 4719-4724, 2019.
11) H. Adachi: On the Theoretical Bases and Application Methods of the Propeller Load Varying Test Method (in Japanese), Journal of the Society of Naval Architects of Japan, No. 154, pp. 109-117, 1983.
12) H. Adachi and M. Hinatsu: On Effective Wake (Consideration Based on the Propeller Load Varying Test Concept), Journal of the Kansai Society of Naval Architects, No. 191, pp. 41-50, 1983.
13) M. Tsujimoto, N. Sogihara, M. Kuroda, K. Kume, and H. Ohba: A Practical Prediction Method for Self-Propulsion Factors in Actual Seas, Proceedings of Twenty-eighth International Offshore and Polar Engineering Conference, pp. 863-870, 2018.
14) A. Yazaki: A diagram to estimate the wake fraction for an actual ship from model tank test, Proceedings of 12th International Towing Tank Conference, pp. 259, 1969.